

Supplementary Information for “Machine Learning Modeling of Temperature-Dependent Optoelectronic Properties of Anharmonic Solid Solutions”

Pol Benítez and Cibrán López

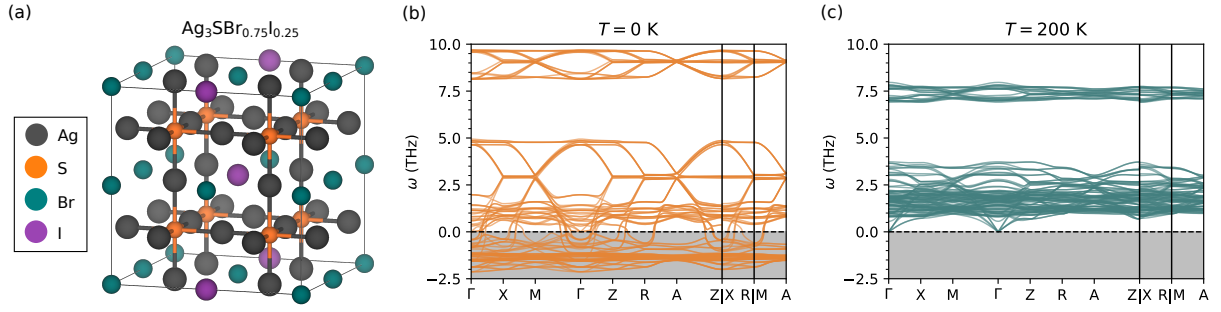
*Department of Physics, Universitat Politècnica de Catalunya, Barcelona 08019, Spain and
Research Center in Multiscale Science and Engineering,
Universitat Politècnica de Catalunya, 08019 Barcelona, Spain*

Edgardo Saucedo

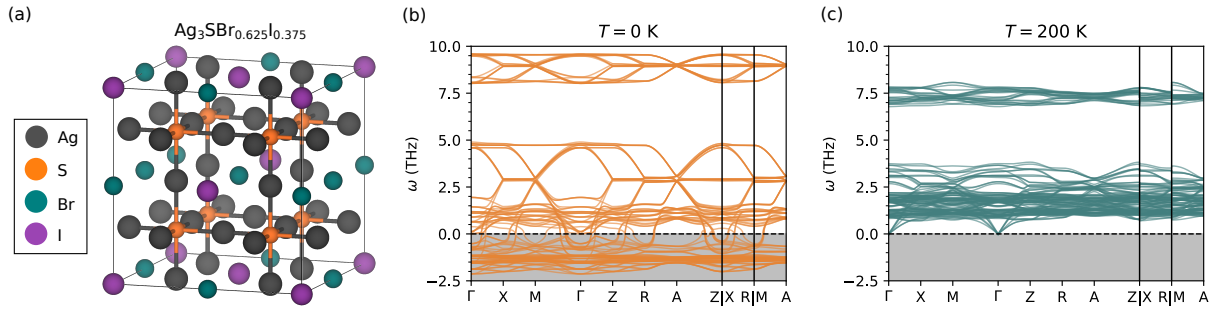
*Research Center in Multiscale Science and Engineering,
Universitat Politècnica de Catalunya, 08019 Barcelona, Spain and
Departament d'Enginyeria Electrònica,
Universitat Politècnica de Catalunya, 08034 Barcelona, Spain*

Claudio Cazorla

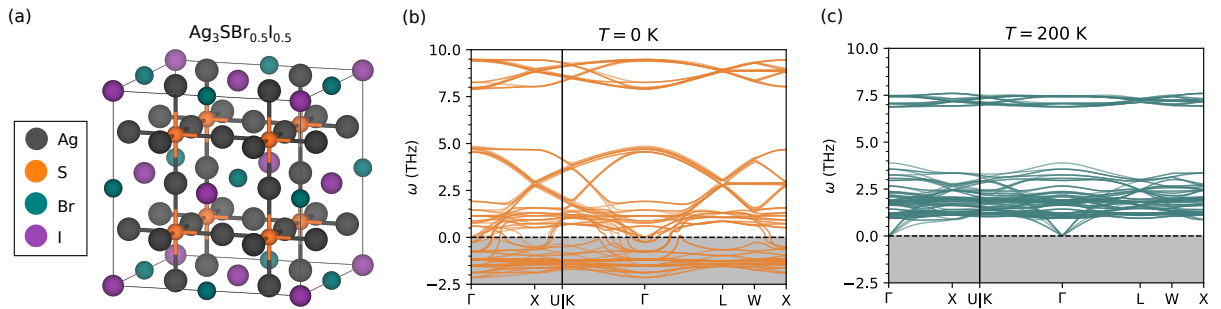
*Department of Physics, Universitat Politècnica de Catalunya, Barcelona 08019, Spain
Research Center in Multiscale Science and Engineering,
Universitat Politècnica de Catalunya, 08019 Barcelona, Spain and
Institució Catalana de Recerca i Estudis Avançats (ICREA),
Passeig Lluís Companys 23, 08010 Barcelona, Spain*



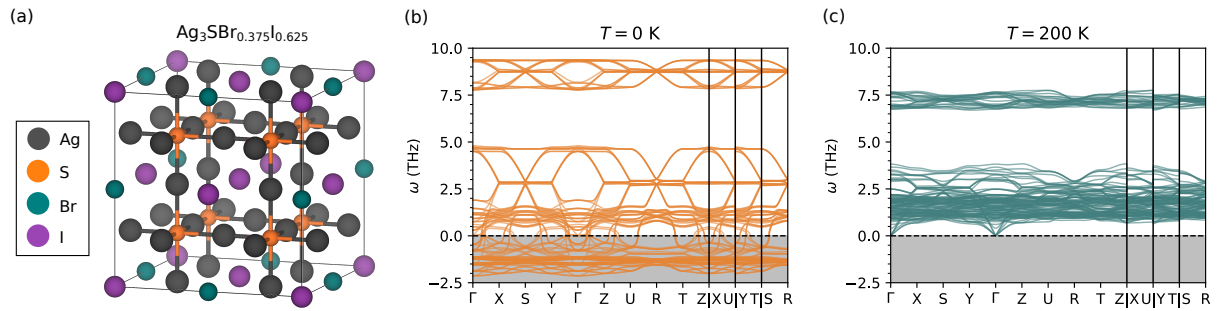
Supplementary Figure 1: (a) Representation of the equilibrium structure determined for the solid solution $\text{Ag}_3\text{SBr}_{0.75}\text{I}_{0.25}$. Phonon dispersions calculated at (b) zero temperature, and (c) at $T = 200 \text{ K}$.



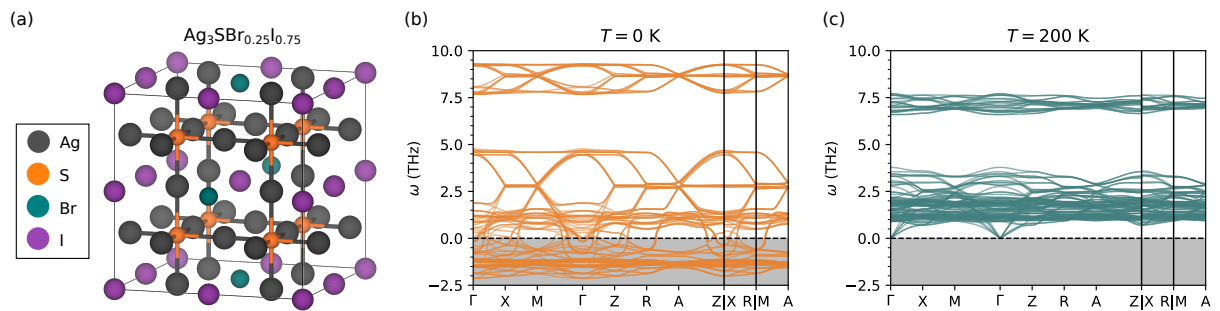
Supplementary Figure 2: (a) Representation of the equilibrium structure determined for the solid solution $\text{Ag}_3\text{SBr}_{0.625}\text{I}_{0.375}$. Phonon dispersions calculated at (b) zero temperature, and (c) at $T = 200 \text{ K}$.



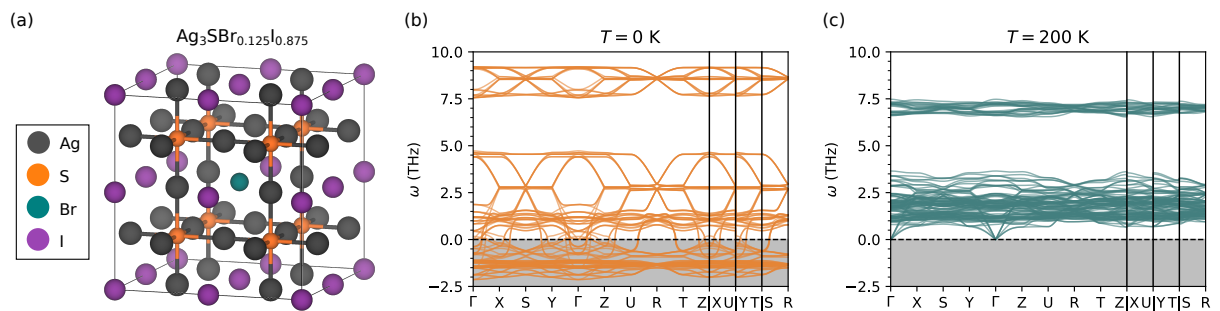
Supplementary Figure 3: (a) Representation of the equilibrium structure determined for the solid solution $\text{Ag}_3\text{SBr}_{0.5}\text{I}_{0.5}$. Phonon dispersions calculated at (b) zero temperature, and (c) at $T = 200 \text{ K}$.



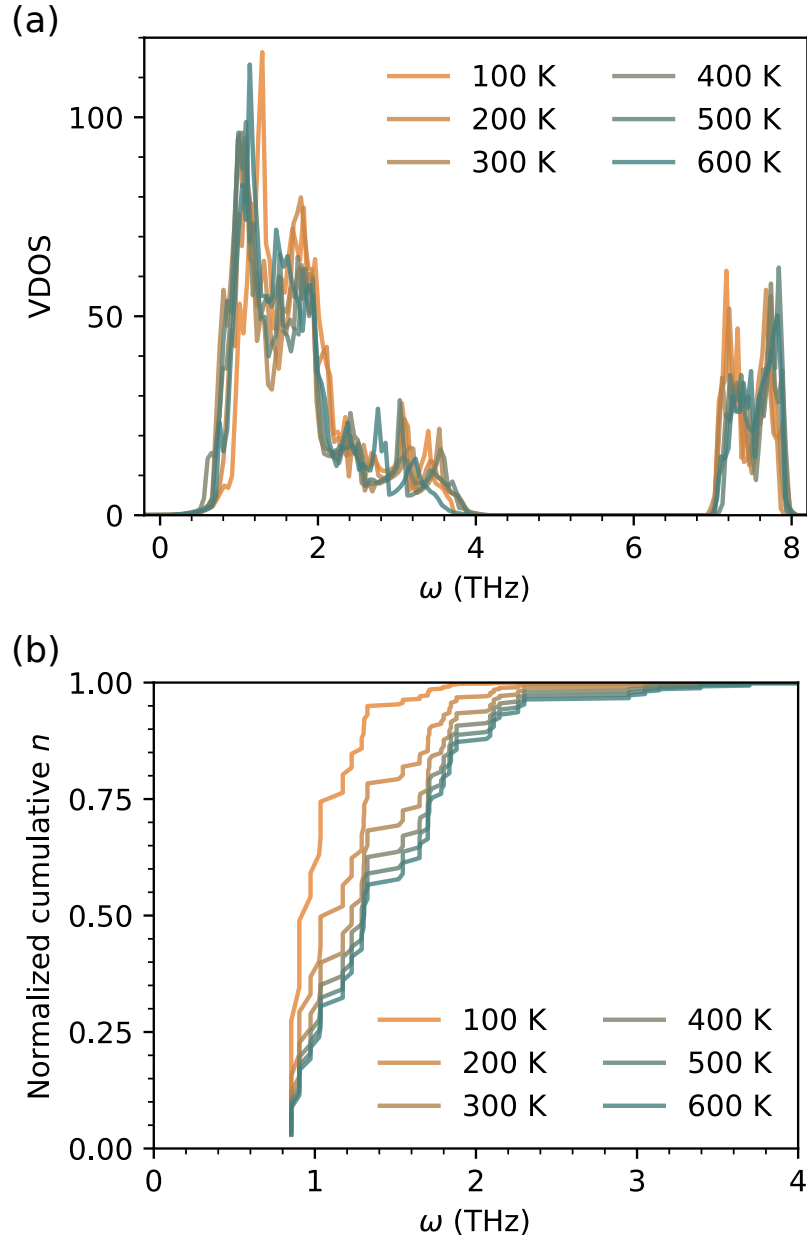
Supplementary Figure 4: (a) Representation of the equilibrium structure determined for the solid solution $\text{Ag}_3\text{SBr}_{0.375}\text{I}_{0.625}$. Phonon dispersions calculated at (b) zero temperature, and (c) at $T = 200 \text{ K}$.



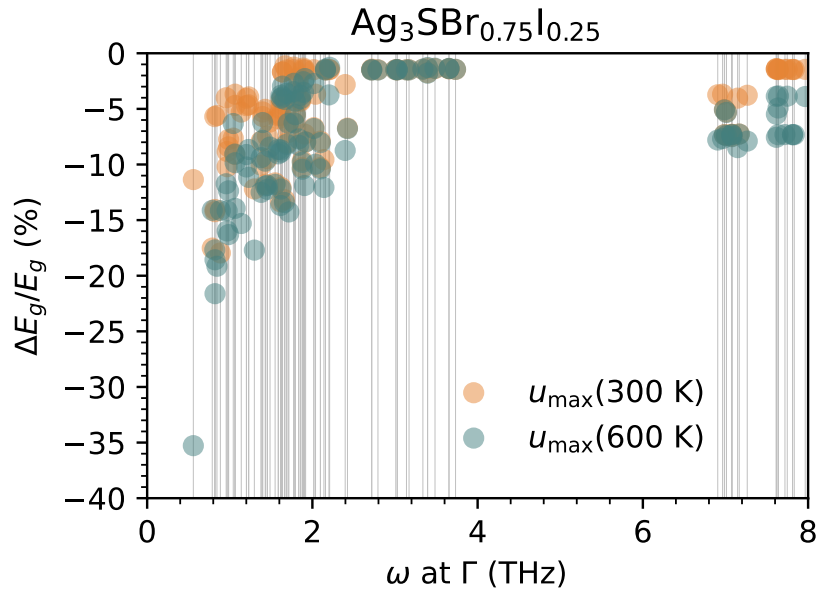
Supplementary Figure 5: (a) Representation of the equilibrium structure determined for the solid solution $\text{Ag}_3\text{SBr}_{0.25}\text{I}_{0.75}$. Phonon dispersions calculated at (b) zero temperature, and (c) at $T = 200 \text{ K}$.



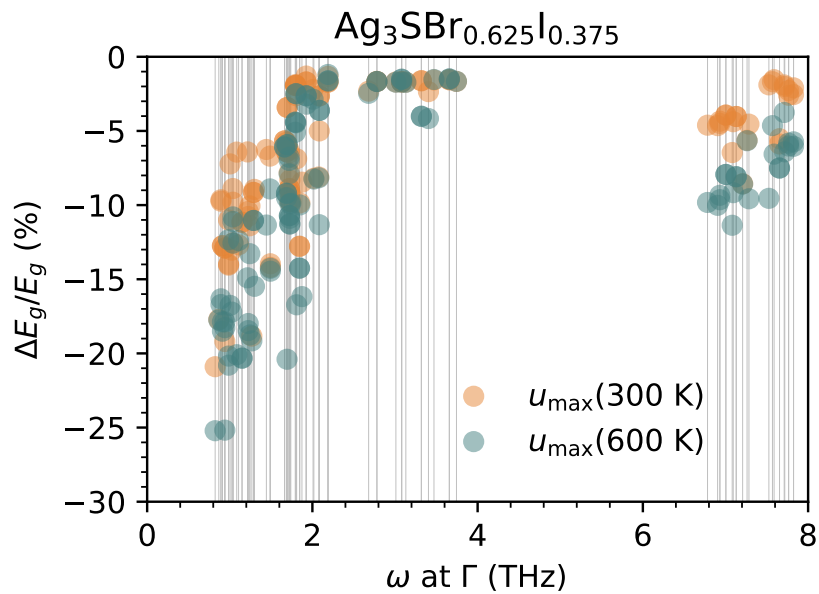
Supplementary Figure 6: (a) Representation of the equilibrium structure determined for the solid solution $\text{Ag}_3\text{SBr}_{0.125}\text{I}_{0.875}$. Phonon dispersions calculated at (b) zero temperature, and (c) at $T = 200 \text{ K}$.



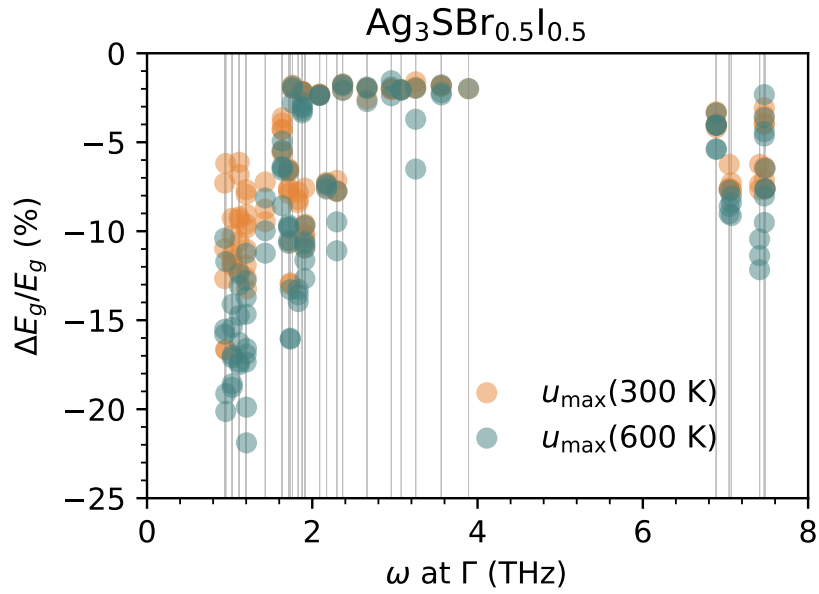
Supplementary Figure 7: (a) Temperature-dependence of the vibrational density of states (VDOS). T -renormalised VDOS were calculated by performing Fourier transform of the velocity autocorrelation function obtained from molecular dynamics simulations. (b) Normalized cumulative VDOS occupation for the solid solution $\text{Ag}_3\text{SBr}_{0.875}\text{I}_{0.125}$ (considering Γ -point phonons only).



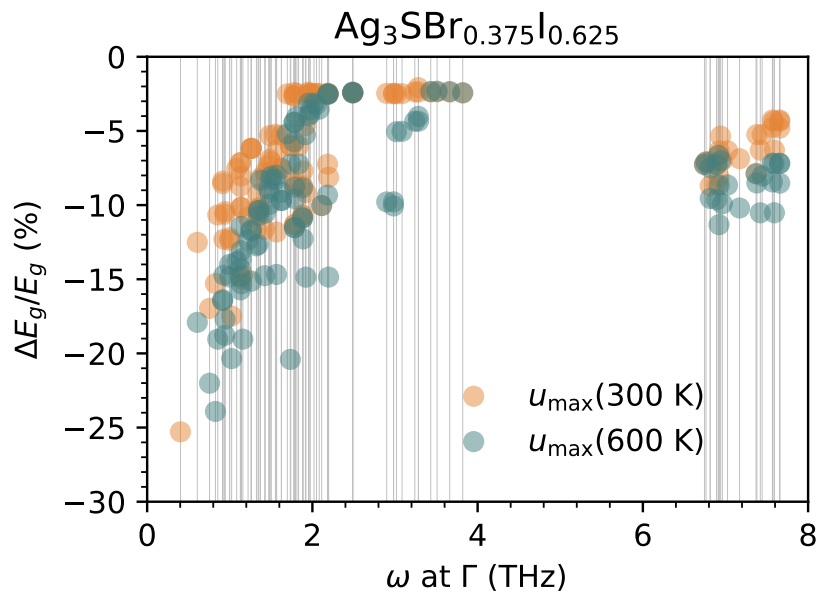
Supplementary Figure 8: Predicted relative band-gap change upon Γ -phonon mode distortions at 300 and 600 K for Ag₃SBr_{0.75}I_{0.25}.



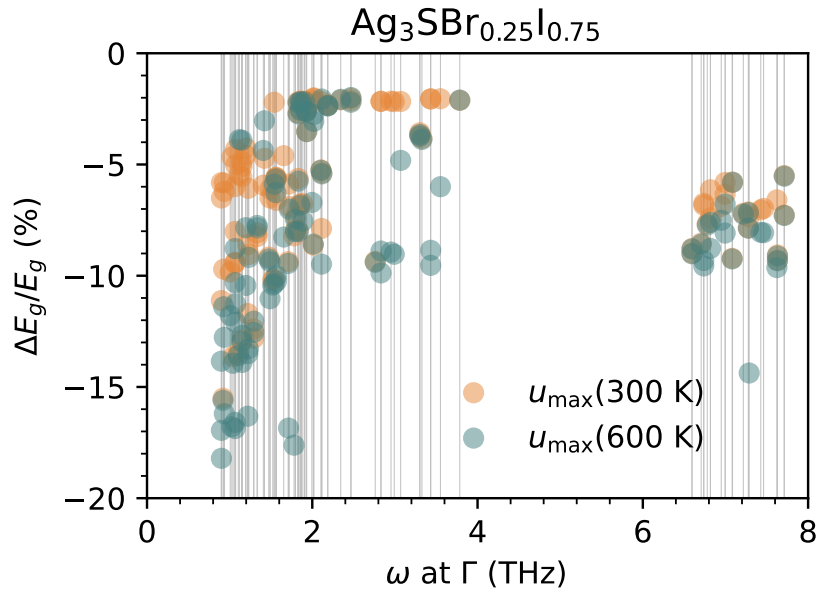
Supplementary Figure 9: Predicted relative band-gap change upon Γ -phonon mode distortions at 300 and 600 K for Ag₃SBr_{0.625}I_{0.375}.



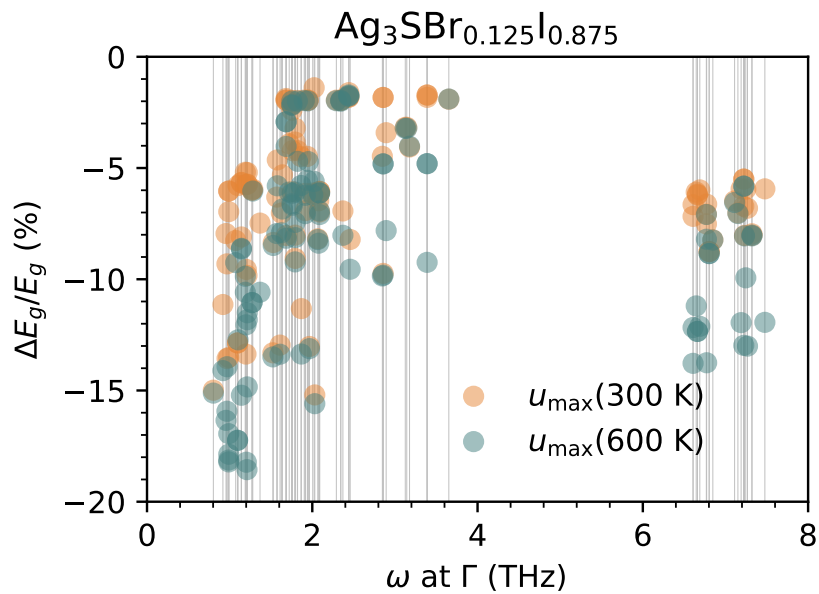
Supplementary Figure 10: Predicted relative band-gap change upon Γ -phonon mode distortions at 300 and 600 K for Ag₃SBr_{0.5}I_{0.5}.



Supplementary Figure 11: Predicted relative band-gap change upon Γ -phonon mode distortions at 300 and 600 K for Ag₃SBr_{0.375}I_{0.625}.



Supplementary Figure 12: Predicted relative band-gap change upon Γ -phonon mode distortions at 300 and 600 K for Ag₃SBr_{0.25}I_{0.75}.



Supplementary Figure 13: Predicted relative band-gap change upon Γ -phonon mode distortions at 300 and 600 K for Ag₃SBr_{0.125}I_{0.875}.

SUPPLEMENTARY DISCUSSION

To calculate the normalized cumulative occupation of vibrational states, $\chi(\omega, T)$, as function of phonon frequency, ω , and temperature, T , we employed the formula (Supplementary Fig. 7):

$$\chi(\omega, T) = \frac{\int_0^\omega g(z, T) n_{\text{BE}}(z, T) dz}{\int_0^\infty g(z, T) n_{\text{BE}}(z, T) dz}, \quad (1)$$

where g is the vibrational density of states (VDOS) and n_{BE} the Bose-Einstein distribution function expressed as:

$$n_{\text{BE}}(\omega, T) = \frac{1}{e^{\frac{\hbar\omega}{k_B T}} - 1}, \quad (2)$$

where \hbar and k_B are the Planck and k_B Boltzmann constants, respectively.

The temperature-dependent VDOS was calculated by performing Fourier transform of the velocity autocorrelation function extracted from long molecular dynamics simulations. High-energy, unoccupied vibrational states do not contribute to the cumulative occupation function (Supplementary Fig. 7). At $T = 0$ K, and neglecting quantum nuclear effects, optical phonon modes are unoccupied, such that $\chi(\omega, 0) = 0$. As the temperature increases, low-frequency optical phonons, which are primarily responsible for the reduction of the band gap in CAP solid solutions (see main text), become progressively populated.